

# Generation of lattice structures of optical vortices

Alexander Dreischuh and Sotir Chervenkov  
*Department of Quantum Electronics, Sofia University,  
5 James Bouchier Blvd., 1164 Sofia, Bulgaria*

Dragomir Neshev  
*Vrije Universiteit Amsterdam, Laser Centre, De Boelelaan 1081, 1081 HV Amsterdam, The Netherlands*

Gerhard G. Paulus  
*Max-Planck-Institut für Quantenoptik, Hans-Kopfermann-Str. 1, D-85748 Garching, Germany*

Herbert Walther  
*Max-Planck-Institut für Quantenoptik, Hans-Kopfermann-Str. 1, D-85748 Garching, Germany  
Ludwig-Maximilians-Universität München, Sektion Physik, Am Coulombwall 1, D-85748 Garching, Germany*

We demonstrate experimentally the generation of square and hexagonal lattices of optical vortices and reveal their propagation in a saturable nonlinear medium. If the topological charges of the vortices are of the same sign the lattice exhibit rotation, while if alternative, we observe stable propagation of the structures. In the nonlinear medium the lattices induce periodic modulation of the refractive index. Diffraction of a probe beam by this nonlinearity-induced periodic structure is observed.

## I. INTRODUCTION

Optical vortices are intriguing objects that attract much attention [1] and display fascinating properties with possible applications in the optical transmission of information, or guiding and trapping of particles. They have a characteristic screw-type phase dislocation [2], which order multiplied by its sign is referred to as a topological charge (TC). The study of optical vortices and more general - phase singularities, suggests not only new directions of fundamental research but also provides links to other branches of physics, as quantum optics [3], superfluidity [4], Bose-Einstein condensates [5,6], and cosmology.

Optical vortices can be generated in several different controllable ways: in lasers with large Fresnel numbers [7], by helical phase plates [8], laser mode converters [9,10], or computer-generated holograms (CGHs) [11]. The method of the CGHs, however, is the most commonly used, since it allows precise control of the vortex position, TC, and possibility for generation of specific patterns of optical vortices.

The propagation dynamics of a single vortex, both in linear and nonlinear media, has been a subject of many researches (see, e.g., [12–14]), whereby also the non-canonical properties of the vortex have been taken into account [15,16]. It has been shown that the vortex position on the background beam is strongly affected by any source of phase and intensity gradients [17–19] and could be controlled by interference with a weak plane-wave [20]. Special attention attract the vortices propagating in a

self-defocusing nonlinear medium (NLM), where they can form an optical vortex soliton (OVS) [21]. (For overview on OVSs see Ref. [1], chapters 7 - 8.) OVSs induce in the medium optical waveguides [22–24] which can guide weak information beams. An OVS was first experimentally generated in Kerr NLM [25] and later in media with other types of nonlinearity: saturable-atomic [26], photorefractive [27], and photovoltaic [28]. Recently an OVS was also observed in a quadratic NLM with defocusing response. However, attention has been paid to avoid the modulational instability of the plane-wave background beam [29].

The propagation of multiple-charged OVSs has also been investigated [30,31]. It was found that they are topologically unstable and decay into vortices of unit charge [32]. The vortices produced by the decay, can arrange themselves in regular patterns (vortex ensembles) while interacting with each other by phase and intensity gradients. The decay of the higher-order vortices obey the general principal of conservation the total angular momentum (AM) of the beam carrying them. Additionally, for a closed region of space the net topological charge must be conserved under continuous evolution provided that no vortices enter or leave the region.

An ensemble of optical vortices exhibits a fluid-like motion [18,33] which strongly depends on the geometrical configuration. The propagation of the simplest vortex ensemble, namely a vortex pair, has been investigated by several groups [17,18,33–35]. In Ref. [34] the rotation of the pair of vortices with equal TCs is controlled by the Gyou phase of the host Gaussian beam. By changing the beam intensity, the position of the beam waist inside the self-defocusing NLM changes, thus changing the an-

gle of the rotation at the output plane. A comparison between the degree of rotation of a vortex pair in linear and nonlinear regime was also performed in Ref. [35]. It was pointed out that the effect of rotation in the nonlinear regime could be more than three times higher than in the linear one. The enhancement is assigned to the nonlinear confinement of the vortex cores, which allows the vortices to propagate as vortex filaments.

Recently the propagation of vortex arrays has been investigated. Such arrays were generated by a bent glass plate [36], or as a result of transverse instability of dark soliton stripes [37–39]. The instability could be enhanced additionally when the dark-soliton stripe interacts with an optical vortex, causing “unzipping” of the stripe [40]. Ensembles of ordered optical vortices have also been investigated in quadratic NLM and are promising for controllable generation of multiple-vortex patterns [41]. The proposed method paves a way for creation of reconfigurable vortex ensembles by means of seeded second-harmonic generation.

Regarding the fluid-like motion of the vortex ensembles, a stationary configuration of vortices was found [33]. It consists of three vortices of equal TC situated in an equilateral triangle and an additional vortex with opposite TC in the center. That configuration was proven to be stable under small displacement of one of the dislocations. However, if the vortices are of higher-order they decay and subsequently form another stationary configuration resembling a part of hexagonal honeycomb lattice. This fact directs attention to the investigation of optical vortex lattices and characterisation of the propagation of the beams they are imposed on.

Up to now lattices of optical vortices propagating in NLM were considered only theoretically. The simplest case of square lattice consisting of vortices with alternative charges was investigated by direct modeling of four of them under periodic boundary conditions [42]. Later, lattices with different geometries imposed on a finite background beam (conditions closer to experimental ones) were considered [33]. It was shown that depending on the TCs the vortex lattices can exhibit rotation or rigid propagation for equal or alternative TCs, respectively. In addition, lattices possess elasticity against displacement of one or more vortices out of their equilibrium positions.

Here we report the first to our knowledge experimental investigation of lattice structures of optical vortices in self-defocusing NLM. We concentrate our attention on two types of lattice geometries - square and hexagonal one. When propagating in the NLM they induce a periodic modulation of its refractive index. For high beam intensities these changes are sufficient to cause a diffraction of a probe beam propagating perpendicularly to the volume with periodically modulated refractive index. This diffraction may be controlled by steering the propagation of the vortex-lattice, e.g. by controlling its

degree of rotation (for lattices consisting of vortices with equal charges). Additional control may be attained by changing the pump beam intensity which changes the refractive index of the medium and therefore the diffraction efficiency of the induced periodic phase grating.

The maximal refractive index change in our experiment is of the order of  $10^{-4}$  to  $10^{-3}$  which is not enough to form an effective two-dimensional photonic band-gap structure [43]. As a proof-of-principle, however, one can consider the possibility to trap glass spheres [44] by the optical vortices ordered in a lattice. This might give an opportunity for generation of effective two-dimensional photonic crystals. Such a crystal could be reconfigured by altering the degree of rotation of the lattice (by changing the intensity of the focused background beam as in Ref. [34]) for equal TCs, or by use of dynamically reconfigurable holograms [45].

We would also like to emphasize the close link between our results and the field of Bose-Einstein condensates, where experimental investigations on vortex ensembles [46], vortex arrays as a result of dark soliton-stripe instability [47], and vortex lattices [48] have been reported recently.

## II. GENERAL ANALYSIS

Let us consider the propagation of a beam in self-defocusing NLM with saturable nonlinearity where its evolution is described by the normalized nonlinear Schrödinger equation (NLSE) for the slowly-varying amplitude envelope

$$i \frac{\partial E}{\partial z} + \frac{1}{2} \Delta_{\perp} E - \frac{|E|^2 E}{(1 + s|E|^2)^{\gamma}} = 0, \quad (1)$$

where  $\Delta_{\perp}$  is the transverse Laplace operator. The transverse coordinates  $(x, y)$  are normalized to the characteristic size of the dark structures  $a$ , and the propagation coordinate  $z$  is normalized to the diffraction length of the dark beams. The background beam intensity  $I = |E|^2$  is expressed in units of the intensity necessary to form one-dimensional (1D) dark soliton  $I_{1Dsol}$  of size  $a$ . The saturation parameter is defined by  $s = I_{1Dsol}/I_{sat}$ , where  $I_{sat}$  is the saturation intensity retrieved by the experimental conditions. The model of the saturation we use is introduced phenomenologically in order to describe the nonlinear response of the thermal medium. It was derived from a test experiment for self-bending of the background beam and described in detail in our previous works [32,49]. The parameters of the nonlinear response function  $s$  and  $\gamma$  depend on the particular realization of the experiment, e.g. the properties of the NLM and the focusing conditions. In all measurements reported here we use thermal nonlinearity, and in particular ethylene-glycol dyed with DODCI (Diethyloxadycarbocyanine io-

dide). Two concentrations of the dye were used so that  $s = 0.4$  and  $1.2$ , respectively and  $\gamma \simeq 3$  in both cases.

In order to investigate the propagation dynamics of vortex lattices we first conducted numerical simulations by use of beam propagation method. The initial conditions were modelled as superposition of vortices situated in the nodes of a lattice:

$$E(\vec{r}, z = 0) = \prod_{j,k=-\infty}^{\infty} \begin{cases} \text{sq}(\vec{r} - \vec{r}_{jk}) \\ \text{hex}(\vec{r} - \vec{r}_{jk}) \end{cases}, \quad (2)$$

with a square and hexagonal symmetry respectively. In Eq. (2)  $\vec{r}_{jk}$  are the nodes of the Bravais lattice representing the physical lattice structure. The square lattice (Fig. 1 - upper row) coincides with its Bravais lattice, however the hexagonal honey-comb lattice (Fig. 1 - second row) is represented by as Bravais lattice with a base containing two vortices. If one define the primitive vectors of the Bravais lattice as  $\vec{b}$  and  $\vec{c}$  then its nodes are described as  $\vec{r}_{jk} = j\vec{b} + k\vec{c}$ , with  $j, k$  integer numbers. The primitive vectors of the square lattice are orthogonal to each other and can be expressed in  $(x, y)$  coordinates as  $\vec{b} = (\Delta, 0)$ ,  $\vec{c} = (0, \Delta)$ , where  $\Delta$  is the distance between two neighbouring vortices. For the honey-comb lattice the primitive vectors are not orthogonal and are expressed as:  $\vec{b} = (\sqrt{3}\Delta, 0)$  and  $\vec{c} = (\frac{\sqrt{3}}{2}\Delta, \frac{3}{2}\Delta)$ . Then the two vortices inside the elementary cell have positions  $\vec{r}_1 = \frac{1}{3}(\vec{b} + \vec{c})$  and  $\vec{r}_2 = \frac{2}{3}(\vec{b} + \vec{c})$ .

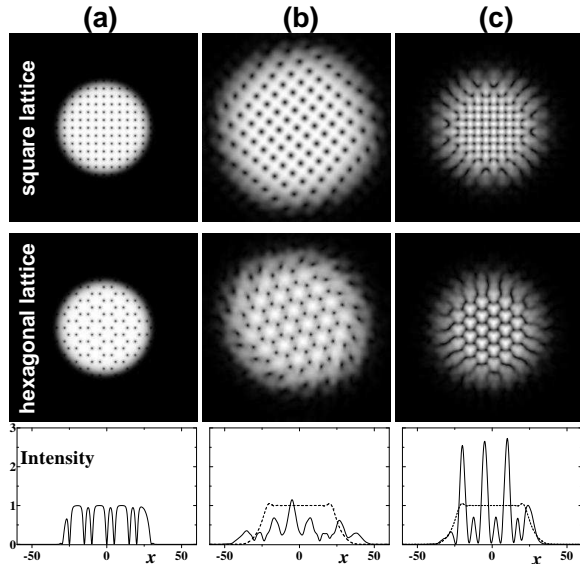


FIG. 1. Background beams containing vortex lattices of different geometries. (a) at the input of the NLM and (b,c) at  $z = 10$  for lattice with equal and alternating TCs, respectively. Upper row: Images of square-shaped lattice; Second row - hexagonal lattice; Bottom row - transverse slices of hexagonal lattices. For comparison, transverse slice of the background beam (without vortices nested in) is shown with dashed curve. In all cases  $\Delta = 5.0$ ,  $I_0 = 1$ , and  $s = 0.4$ . The images are grayscale-coded and white corresponds to the maximal intensity.

The functions  $\text{sq}(\vec{r} - \vec{r}_{jk})$  and  $\text{hex}(\vec{r} - \vec{r}_{jk})$  describe the structure of the elementary cell of the Bravais lattice and are expressed as:

$$\text{sq}(\vec{r} - \vec{r}_{jk}) = \tanh(|\vec{r} - \vec{r}_{jk}|) \exp \left[ i \text{sgn}^{j+k} \arctan \frac{(\vec{r} - \vec{r}_{jk})_y}{(\vec{r} - \vec{r}_{jk})_x} \right], \quad (3)$$

and

$$\text{hex}(\vec{r} - \vec{r}_{jk}) = \tanh(|\vec{r} - \vec{r}_{jk} - \vec{r}_1|) \tanh(|\vec{r} - \vec{r}_{jk} - \vec{r}_2|) \times \exp \left[ i \arctan \frac{(\vec{r} - \vec{r}_{jk} - \vec{r}_1)_y}{(\vec{r} - \vec{r}_{jk} - \vec{r}_1)_x} \right] \exp \left[ i \text{sgn} \arctan \frac{(\vec{r} - \vec{r}_{jk} - \vec{r}_2)_y}{(\vec{r} - \vec{r}_{jk} - \vec{r}_2)_x} \right].$$

The sign function  $\text{sgn}$  is equal to  $+1$  for equal TCs and  $-1$  for alternative ones.

Then the lattice structure is imposed on a super-Gaussian (flat-top) background beam

$$B(x, y, z = 0) = \sqrt{I_0} \exp \left\{ - \left( \sqrt{\frac{x^2 + y^2}{w^2}} \right)^{14} \right\}, \quad (5)$$

where the width  $w$  is chosen to exceed the characteristic width of the dark structures  $a$  more than 40 times, and  $I_0$  is the maximal background beam intensity.

We modelled the propagation of lattices of different geometries and different TC distributions (see Fig. 1). No qualitative differences were observed in the propagation of vortex-structures with respect to the lattice geometry (square or hexagonal). The mode of propagation, however, crucially depends on the vortex charge distribution (equal - Fig. 1b or alternative - Fig. 1c). Two characteristic differences are clearly seen: (i) In the case of equal TCs ( $\text{sgn} = +1$ ) the superposition of the phases of all vortices results in azimuthal phase gradient and nonzero total AM which causes rotation of the whole structure (Fig. 1b). In the case of alternative TCs ( $\text{sgn} = -1$ ) the superposition of all the phases gives, in average, no phase gradient and zero total AM. As a result, steady propagation of the lattice is observed in the simulations (Fig. 1c); (ii) In the case of equal TCs the non-zero total AM and the centrifugal forces lead to increased broadening of the background beam. The maximal intensity rapidly decreases along the NLM ( $I \simeq 0.6$  at  $z = 10$  Fig. 1b - bottom row). The dependence on the intensity of the background beam in this case is relatively weak and the topological effects dominate the nonlinear ones. In the case of alternative TCs (Fig. 1c) the background beam broadening is an effect only due to the combined action of the diffraction and self-defocusing nonlinearity and depends on the intensity.

The degree of rotation of both lattice geometries for the case of equal TCs is depicted in Fig. 2. The rotation is due to the phase gradient, which is higher for the denser (square-shaped) structure. Therefore its rotation

(open squares in Fig. 2) is faster than the rotation of the hexagonal one (solid circles). The dependence on the distance is not linear because in the course of propagation the background beam spreads out and the distance between the vortices increases. That causes a decrease of the angular velocity with the propagation length.

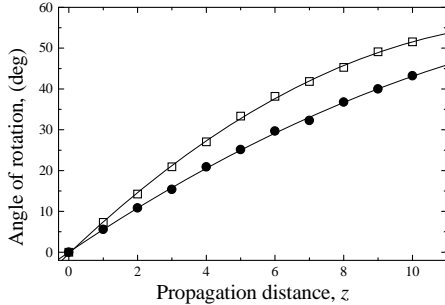


FIG. 2. Angle of rotation of vortex lattices of equal TCs vs. propagation distance for square (open squares) and hexagonal (solid circles) geometry. The solid lines are drawn to guide the eye. The lattice parameters are the same as in Fig. 1.

Similar behaviour was previously described for the case of Kerr nonlinearity [33]. Here we would like to point out the features caused by the saturation of the nonlinearity. As already mentioned, the rotation of the lattice and the increased beam spreading in the case of equal TCs are topological effects. The effects which depend on the nonlinearity are related to the local intensity via the specific beam shape and the vortex-pattern formed on the background. For example, the transverse profile of a single OVS in saturable medium differs significantly at different values of the saturation parameter [26] (the OVS is broader at higher saturation). In the case of periodically ordered vortices when each individual dark beam starts to broaden, the overlapping with the wings of its neighbours increases, while the individual cores do not change significantly. Since the vortices are imposed on a finite background beam and its total energy is conserved, bright peaks form in between as a result of local energy redistribution (See Fig. 1c - bottom row). Therefore, even in saturable medium the well defined periodic modulation of the refractive index of the medium is still preserved.

### III. EXPERIMENTAL INVESTIGATION

The experimental setup is similar to the one used in our previous works [32,49] and is shown in Fig. 3. The 488nm line from an  $Ar^+$  laser is used to reconstruct the photolithographically produced CGH with the desired vortex-lattice. The +1 (or -1) order of the diffraction is separated by an iris diaphragm (D) and is focused on the input face of a glass cell containing the NLM. The output face of the cell is imaged to a CCD camera, and

neutral filters (F) are used to avoid its saturation.

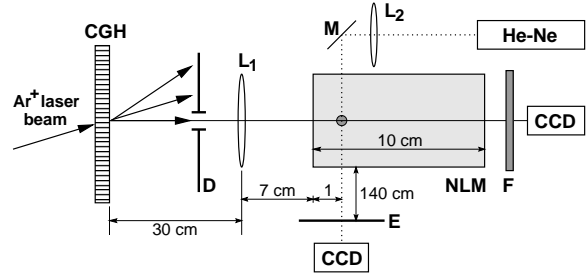


FIG. 3. Experimental setup: CGH - computer generated hologram; D - iris diaphragm;  $L_1$ ,  $L_2$  lenses of focal length 7.0cm and 8.0cm, respectively; M - mirror; E - screen; NLM - nonlinear medium; F - neutral filters; CCD - camera. The characteristic distances are shown.

To assure the correct generation of the lattices by the CGHs we first opened the diaphragm allowing the +1 diffraction order to interfere with the plane zeroth one. Interference patterns for three different cases are presented in Fig. 4. The vortices appear as forks of interference lines. Two neighbouring vortices at each image are marked with arrows. The images show correctly reproduced square-shaped lattice with alternative TCs and two hexagonal lattices with alternative and equal TCs, respectively (Fig. 4, left to right). The images are brighter in the right-hand side since they overlap inhomogeneously with the zeroth order beam. That inhomogeneity also introduces an intensity gradient in the structure of vortices, which causes shrinking and vortex displacement from their regular positions. In overall that leads to deformation of the lattice. Being aware of this fact in the experiment we preserved the regular lattice structure by placing the diaphragm as close as possible to the CGH.

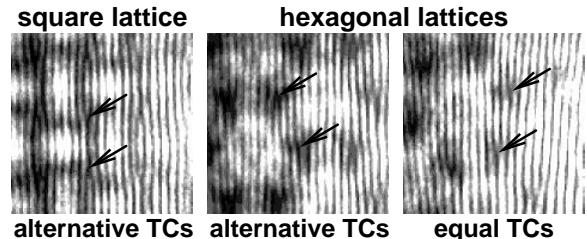


FIG. 4. Interferograms of three experimentally generated lattices. From left to right: square lattice with alternative TCs; hexagonal lattice with alternative TCs; and hexagonal lattice with equal TCs. Two neighbouring vortices in each image are marked with arrows.

The features of the nonlinear propagation are determined by measuring the characteristic nonlinear parameters of the media for the two concentrations of the dye. For the lower one, the power necessary to form a 1D dark-soliton stripe was estimated to be  $P_{1Dsol} \simeq 22mW$  and the saturation power was  $P_{sat} \simeq 60mW$  (measured in a self-bending scheme) [49]. For the higher concen-

tration the characteristic powers were  $P_{1Dsol} \simeq 20mW$  and  $P_{sat} \simeq 16mW$ . The intensity distributions for two hexagonal lattices (with alternative and equal charges) at the end of the NLM with lower dye concentration are shown in Fig. 5. Because of some technical restrictions in synthesizing the CGH, for the lattice with equal TCs, the number of vortices encoded is less than in the hologram with alternative TCs. The geometrical characteristics (the elementary cell of the lattices), however, are the same in both cases. The propagation behaviour for both lattices is clearly different. While the lattice with alternative charges exhibits steady propagation (Fig. 5a) the one with equal ones (Fig. 5b) tends to rotate (at about  $28^\circ$  counter-clockwise). The background beam spreads stronger than in the case of a lattice with alternative charges. Unfortunately, due to the different number of vortices, this fact is not obvious in Fig. 5. The smaller number of vortices in Fig. 5b modulates the background beam in a way that more filters were used to avoid the saturation of the CCD camera. As a consequence, the wings of the background beam in Fig. 5b are not seen and the beam diameter seems to be smaller as compared to Fig. 5a. In order to illustrate that the spreading is indeed higher in the case of equal TCs we looked in detail on the size of the elementary cell of the honey-comb lattice. Since the distances between the neighbouring vortices were encoded in the CGHs to be the same (the produced holograms were inspected by a microscope) any difference in the vortex separation is due to the evolution during propagation. In each image in Fig. 5 we inset the exact size and orientation of the elementary hexagonal cell of the lattice (see bottom-right corner of each image). Indeed the comparison between the elementary cells of the lattices in both cases shows 18% bigger size for the one with equal TCs.

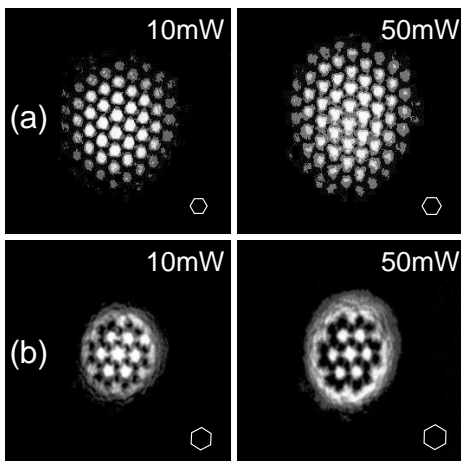


FIG. 5. Experimental images of the vortex lattices after  $10cm$  propagation in the NLM. (a) - hexagonal lattice with alternating TCs for powers of  $10mW$  and  $50mW$ . (b) - hexagonal lattice with equal TCs for the same powers. The insets in each image represent the size and the orientation of the elementary cell of each lattice.

The influence of the nonlinearity can be seen if the corresponding images for two particular powers are compared. We note again that the increase of the beam power does not influence the degree of rotation of the lattice presented in Fig. 5b since the waist of the laser beam is near the input face of the NLM. The higher power of the laser beam contributes, however, to the background beam broadening. Comparing the size of the elementary cell of the same lattice at two different powers we estimated 15% broadening of the beam for the case in Fig. 5a and 12% for the case in Fig. 5b. That difference we attribute to the increased background beam size at the entrance of the NLM, which is due to the topological interaction of the equally charged vortices between the CGH and the NLM.

The square-shaped lattices were investigated in the same way and qualitatively similar features were observed. We also investigated lattices with intentionally encoded defects in their structure, e.g. when one of the vortices is missing or all of the vortices in a line are shifted out of their equilibrium position. These experiments revealed the interesting property that the lattices exhibit elasticity. However the resolution in our experiments was not sufficient to resolve this feature in more than qualitative manner.

#### IV. DIFFRACTION OF A PROBE BEAM BY VORTEX LATTICES

When an intense laser beam propagates along a NLM its refractive index changes proportionally to the intensity distribution. Since the vortex-lattices possess a periodic intensity distribution (see Fig. 1 and Fig. 5) one can expect periodic modulation of the refractive index. In a self-defocusing medium the higher local intensity will correspond to lower local refractive index. The lattices are imposed on a finite background beam and as whole it induces in the NLM a cylindrical defocusing lens (considered in a perpendicular direction), which is modulated by the dark vortex structure composing the lattice. In a thermal NLM, as slightly absorbing liquid, the nonlocal effect coming from the heat transfer also influence the refractive index change and effectively decreases its modulation. The nonlocality is not taken into account in the model of Eq. (1). Its main influence is that at zero intensity (the points of vortex-phase dislocation) the refractive index change is non-zero (see a description in Ref. [50]).

To investigate the modulation of the refractive index in the NLM caused by the presence of lattices we conducted an experiment in which a (probe) single-mode He-Ne laser beam was directed perpendicularly to then (pump)  $Ar^+$  laser beam, as shown in Fig. 3. We aligned the probe beam in a way to cross the pump one  $1cm$  inside the NLM. (The higher dye concentration was used in this experiment). The input profile of the He-Ne laser

beam is shown in Fig. 6a and its circular symmetry is evident. When it crosses the  $\text{Ar}^+$  laser beam the symmetry is distorted and the beam elongates in direction perpendicular to the plane of Fig. 3.

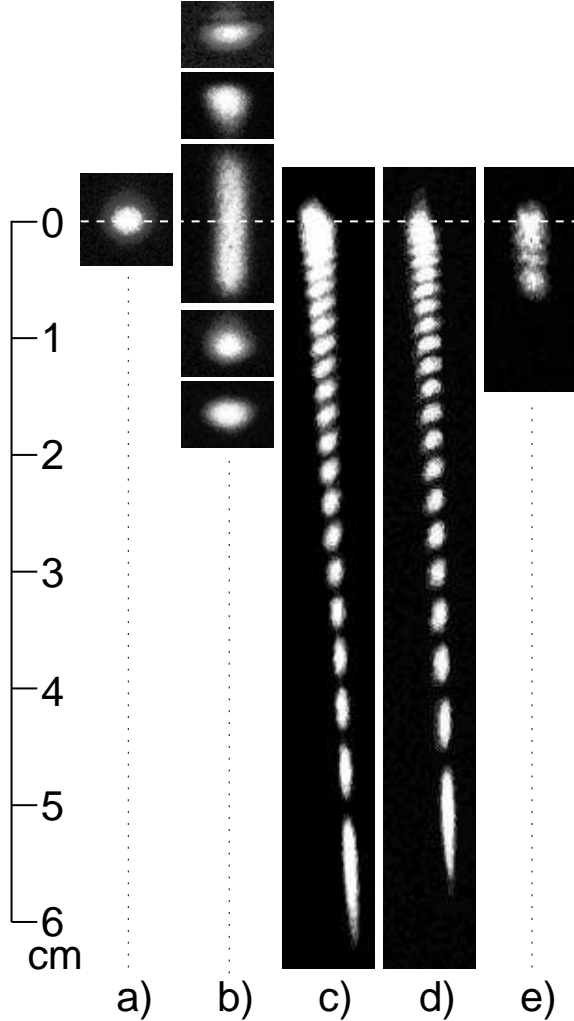


FIG. 6. Images of the probe He-Ne beam on the screen E. (a) the input He-Ne laser beam; (b) the intensity profile of the probe beam at low pump power ( $10mW$ ) for different parallel vertical displacements with respect to the pump one; (c), (d) diffraction of the He-Ne beam from the periodic phase gratings induced in the NLM by square and hexagonal lattices, respectively (pump power  $80mW$ ); (e) the diffraction pattern when a single vortex is imposed on the pump beam (pump power  $30mW$ ).

First we identified the effect of optically-induced Gaussian cylindrical lens on the probe beam. In order to keep the same background beam characteristics the CGH was shifted in a way that only a region with parallel interference lines was illuminated thus ensuring unmodulated background beam. This unmodulated pump beam induces a cylindrical lens in the NLM whereas the probe one passes through the lens and defocuses (Fig. 6b - central image). The diameters of both beams were estimated to be approximately equal at the cross point. Therefore one

should expect that the probe beam will be strongly affected by aberrations of the induced lens. In Fig. 6b five probe beam profiles are shown for different positions of the He-Ne laser beam. The pump power is kept  $10mW$ . Different input positions of the probe beam are achieved by parallel vertical translation by a simple periscopic system denoted for simplicity as mirror M in Fig. 3. The He-Ne beam elongates symmetrically if it crosses the pump in the center and asymmetrically if it is shifted up or down. At higher powers the aberration of the induced cylindrical lens becomes vertically asymmetric, probably due to the asymmetric heat diffusion in the cell.

The situation is different when the vortex-lattice is imposed on the background beam. At power of the  $\text{Ar}^+$  laser beam higher than  $20mW$  the vortices have well confined cores. Due to the nonlinear change of the refractive index the vortex lattice ‘writes’ a phase grating in the NLM. The perpendicularly propagating He-Ne laser beam passes through this grating and develops well pronounced diffraction orders at the output screen as seen in Fig. 6c,d at  $80mW$  pump power. The constant of the phase grating written is apparently different for the square-shaped lattice (Fig. 6c) and for the hexagonal-shaped one (Fig. 6d). In the first case the period of the vortex-structure is smaller (so this of the phase grating) and higher dispersion in the diffraction orders is observed (higher angle of diffraction). At lower powers diffraction orders were also observed. However, it was more difficult to distinguish them at the screen (E) because the effective cylindrical lens had larger focal length. At different powers the magnitude of the refractive index changes and the modulation depth of the phase grating written in the NLM is different. This influences the energy redistribution between the diffraction orders. Moreover, because of the finite number of the vortices in the lattices and the nearly equal sizes of the pump and the probe beams the diffraction from the phase grating couldn’t be compared directly with the diffraction from an infinite periodic structure. In our opinion the ratio between the intensities of the different diffraction orders is gradually influenced by the fact that different parts of the probe beam pass through different number of vortices. Further, at the exit of the phase grating, the modulated probe beam is additionally affected by the aberration of the thermal lens.

To assure that the observed diffraction structure is really induced by the periodicity of the vortex lattices we tested the diffraction caused by a single vortex imposed on the background beam. As seen in Fig. 6e the diffraction by a single vortex is substantially different and resembles the diffraction of a laser beam by a wire. In all our experiments we observed strong vertical asymmetry of the probe-beam diffraction pattern, which always developed downwards at higher powers. Numerical modeling of the processes and further experimental investigations should allow to gain deeper insight in the relative

strength of the mentioned mechanisms.

## V. CONCLUSION

In conclusion, we successfully generated experimentally lattice structures of optical vortices with different topological charge distribution and described their propagation in saturable NLM. Due to the intensity dependence of the refractive index these lattices induce periodic modulation of the refractive index of the medium and ‘write’ and effective phase grating in it. The modulation is sufficient to force a perpendicularly propagating probe beam of a He-Ne laser to diffract. This feature could appear as an interesting possibility to create periodic structures in the refractive index of a NLM. It could find an application for optical writing of two-dimensional photonic crystals and could appear relevant to the physics of Bose-Einstein condensates.

## VI. ACKNOWLEDGEMENTS

A.D. thanks the Alexander-von-Humboldt foundation for the awarded fellowship and for the possibility to carry out the measurements at the Max-Planck-Institut für Quantenoptik (Garching, Germany). The work of D.N. was partially supported by Marie-Curie Individual Fellowship under contract HPMFCT-2000-00455. The authors thank to Yu. Kivshar, L. Torner, A. Desyatnikov, and N. Herschbach for the valuable discussions and the support of this work.

- 
- [1] See, e.g., M. Vasnetsov and K. Staliunas (Eds.), *Optical Vortices* (Nova Sci. Publ., New York, 1999).
- [2] J.F. Nye and M.V. Berry, “Dislocations in wave trains,” *Proc. R. Soc. London Ser. A* **336**, 165-190 (1974).
- [3] A. Mair and A. Zeilinger, “Entangled states of orbital angular momentum of photons,” In *Epistemological and Experimental Perspectives on Quantum Physics* 249-252 (1999).
- [4] See, e.g., R.J. Donnelly, *Quantized Vortices in Helium II* (Cambridge University Press, Cambridge, 1991).
- [5] J.E. Williams and M.J. Holland, “Preparing topological states of a Bose-Einstein condensate,” *Nature* **401**, 568-572 (1999).
- [6] M.R. Matthews, B.P. Anderson, P.C. Haljan, D.S. Hall, C.E. Wieman, and E.A. Cornell, “Vortices in a Bose-Einstein condensate,” *Phys. Rev. Lett.* **83**, 2498-2501 (1999).
- [7] P. Coullet, L. Gil, F. Rocca, “Optical vortices,” *Opt. Commun.* **73**, 403-408 (1989).
- [8] M.W. Beijersbergen, R.P.C. Coerwinkel, M. Kristiasen, and J.P. Woerdman, “Helical-wave-front laser-beams produced with a spiral phaseplate,” *Opt. Commun.* **112**, 321-327 (1994).
- [9] Chr. Tamm and C.O. Weiss, “Bistability and optical switching of spatial patterns in a laser,” *J. Opt. Soc. B* **7**, 1034-1038 (1990).
- [10] D.V. Petrov, F. Canal, and L. Torner, “A simple method to generate optical beams with a screw phase dislocation,” *Opt. Commun.* **143**, 265-267 (1997).
- [11] N.R. Heckenberg, R. McDuff, C.P. Smith, A.G. White, “Generation of optical phase singularities by computer-generated holograms,” *Opt. Lett.* **17**, 221-223 (1992).
- [12] I.V. Basisty, V.Y. Bazhenov, M.S. Soskin, and M.V. Vasnetsov, “Optics of light beams with screw dislocations,” *Opt. Commun.* **103**, 422-428 (1993).
- [13] I. Freund, “Critical point explosions in two-dimensional wave fields,” *Opt. Commun.* **159**, 99-117 (1999).
- [14] K. Staliunas, “Vortices and dark solitons in two-dimensional nonlinear Schrödinger equation,” *Chaos, Solitons Fractals* **4**, 1783-1796 (1994).
- [15] G. Molina-Terriza, E.M. Wright, and L. Torner, “Propagation and control of noncanonical optical vortices,” *Opt. Lett.* **26**, 163-165 (2001).
- [16] G. Molina-Terriza, J. Recolons, J.P. Torres, L. Torner, and E.M. Wright, “Observation of the dynamical inversion of the topological charge of an optical vortex,” *Phys. Rev. Lett.* **87**, 023902 (2001).
- [17] D. Rozas, C.T. Law, and G.A. Swartzlander Jr., “Propagation dynamics of optical vortices,” *J. Opt. Soc. Am. B* **14**, 3054-3065 (1997).
- [18] D. Rozas, Z. S. Sacks, and G. A. Swartzlander, Jr., “Experimental observation of fluidlike motion of optical vortices,” *Phys. Rev. Lett.* **79**, 3399-3402 (1997).
- [19] Yu.S. Kivshar, J. Christou, V. Tikhonenko, B. Luther-Davies, and L.M. Pismen, “Dynamics of optical vortex solitons,” *Opt. Commun.* **152** 198-206 (1998).
- [20] J. Christou, V. Tikhonenko, Y.S. Kivshar, and B. Luther-Davies, “Vortex soliton motion and steering,” *Opt. Lett.* **21**, 1649-1651 (1996).
- [21] Yu.S. Kivshar and B. Luther-Davies, “Dark optical solitons: physics and applications,” *Phys. Rep.* **298**, Ch.7 172-185 (1998).
- [22] A.W. Snyder, L. Poladian, and D.J. Mitchell, “Stable dark self-guided beams of circular symmetry in a bulk Kerr medium,” *Opt. Lett.* **17**, 789-791 (1992).
- [23] A.H. Carlsson, J.N. Malmberg, D. Anderson, M. Lisak, E.A. Ostrovskaya, T. Alexander, and Yu.S. Kivshar, “Linear and nonlinear waveguides induced by optical vortex solitons,” *Opt. Lett.* **25** 660-662 (2000).
- [24] C.T. Law, X. Zhang, and G.A. Swartzlander, Jr., “Waveguiding properties of optical vortex solitons,” *Opt. Lett.* **25**, 55-57 (2000).
- [25] G.A. Swartzlander, Jr. and C.T. Law, “Optical vortex solitons observed in Kerr nonlinear media,” *Phys. Rev. Lett.* **69**, 2503-2506 (1992).
- [26] V. Tikhonenko, Yu.S. Kivshar, V.V. Steblina, A.A. Zozulya, “Vortex solitons in a saturable optical medium,” *J. Opt. Soc. Am. B* **15**, 79-86 (1998).
- [27] G. Duree, M. Morin, G. Salamo, M. Segev, B. Crosignani, P. Di Porto, E. Sharp, and A. Yariv, “Dark photorefrac-

- tive spatial solitons and photorefractive vortex solitons,” *Phys. Rev. Lett.* **74**, 1978-1981 (1995).
- [28] Z. Chen and M. Segev, “Self-trapping of an optical vortex by use of the bulk photovoltaic effect,” *Phys. Rev. Lett.* **78**, 2948-2951 (1997).
- [29] P. Di Trapani, W. Chinaglia, S. Minardi, A. Piskarskas, and G. Valiulis, “Observation of quadratic optical vortex solitons,” *Phys. Rev. Lett.* **84**, 3843-3846 (2000).
- [30] A.V. Mamaev, M. Saffman, and A.A. Zozulya, “Decay of high order optical vortices in anisotropic nonlinear optical media,” *Phys. Rev. Lett.* **78**, 2108-2111 (1997).
- [31] I. Velchev, A. Dreischuh, D. Neshev, and S. Dinev, “Multiple-charged optical vortex solitons in bulk Kerr media,” *Opt. Commun.* **140**, 77-82 (1997).
- [32] A. Dreischuh, G.G. Paulus, F. Zacher, F. Grabson, D. Neshev, and H. Walther, “Modulational instability of multiple-charged optical vortex solitons under saturation of the nonlinearity,” *Phys. Rev. E* **60**, 7518-7524 (1999).
- [33] D. Neshev, A. Dreischuh, M. Assa, and S. Dinev, “Motion control of ensembles of ordered optical vortices generated on finite extent background,” *Opt. Commun.* **151**, 413-421 (1998).
- [34] B. Luther-Davies, R. Powles, V. Tikhonenko, “Nonlinear rotation of three-dimensional dark spatial solitons in a Gaussian laser beam,” *Opt. Lett.* **19**, 1816-1818 (1994).
- [35] D. Rozas and G.A. Swartzlander, Jr., “Observed rotational enhancement of nonlinear optical vortices,” *Opt. Lett.*, **25**, 126-128 (2000).
- [36] G.-H. Kim, J.-H. Jeon, Y.-Ch. Noh, K.-H. Ko, H.-J. Moon, J.-H. Lee, and J.-S. Chang, “An array of phase singularities in a self-defocusing medium,” *Opt. Commun.* **147**, 131-137 (1998).
- [37] G.M. McDonald, K.S. Syed, and W.J. Firth, “Dark spatial soliton break-up in the transverse plane,” *Opt. Commun.* **95** 281-288 (1993).
- [38] V. Tikhonenko, J. Christou, B. Luther-Davies, and Yu.S. Kivshar, “Observation of vortex solitons created by the instability of dark soliton stripes,” *Opt. Lett.* **21**, 1129-1131 (1996).
- [39] A.V. Mamaev, M. Saffman, and A.A. Zozulya, “Propagation of dark stripe beams in nonlinear media: Snake instability and creation of optical vortices,” *Phys. Rev. Lett.* **76**, 2262-2265 (1996).
- [40] D. Neshev, A. Nepomnyashchy, and Yu.S. Kivshar, “Nonlinear Aharonov-Bohm scattering for optical vortices,” *Phys. Rev. Lett.* **87**, 043901 (2001).
- [41] G. Molina-Terriza and L. Torner, “Reconfigurable dynamic beam shaping in seeded frequency doubling,” *Opt. Lett.* **26** 154-156 (2001).
- [42] G.S. McDonald, K.S. Syed, and W.J. Firth, “Optical vortices in beam propagation through a self-defocusing medium,” *Opt. Commun.* **94**, 469-476 (1992).
- [43] S.W. Leonard, J.P. Mondia, H.M. van Driel, O. Toader, S. John, K. Busch, A. Birner, U. Gösele, and V. Lehmann, “Tunable two-dimensional photonic crystals using liquid-crystal infiltration,” *Phys. Rev. B* **61**, R2389-R2392 (2000).
- [44] K.T. Gahagan, G.A. Swartzlander, Jr., “Optical vortex trapping of particles,” *Opt. Lett.* **21**, 827-829 (1996).
- [45] Ch. Slinger, P. Brett, V. Hui, G. Monnington, D. Pain, and I. Sage, “Electrically controllable multiple, active, computer-generated hologram,” *Opt. Lett.* **22**, 1113-1115 (1997).
- [46] K.W. Madison, F. Chevy, W. Wohlleben, and J. Dalibard, “Vortex Formation in a Stirred Bose-Einstein Condensate,” *Phys. Rev. Lett.* **84**, 806-809 (2000).
- [47] B.P. Anderson, P.C. Haljan, C.A. Regal, D.L. Feder, L.A. Collins, C.W. Clark, and E.A. Cornell, “Watching dark solitons decay into vortex rings in a Bose-Einstein condensate,” *Phys. Rev. Lett.* **86**, 2926-2929 (2001).
- [48] J.R. Abo-Shaeer, C. Raman, J.M. Vogels, W. Ketterle, “Observation of vortex lattices in Bose-Einstein condensates,” *Science* **292**, 476-479 (2001).
- [49] A. Dreischuh, D. Neshev, G.G. Paulus, and H. Walther, “Experimental generation of steering odd dark beams of finite length,” *J. Opt. Soc. Am. B* **17**, 2011-2017 (2000).
- [50] A.M. Deykoon and G.A. Swartzlander, Jr., “Pinched optical-vortex soliton,” *J. Opt. Soc. Am. B* **18**, 804-810 (2001).